# The performance of the WIYN fiber-fed MOS system — Hydra

Samuel C. Barden, Taft Armandroff

Kitt Peak National Observatory, National Optical Astronomy Observatories*
P.O. Box 26732, Tucson, Arizona 85726-6732

## ABSTRACT

The KPNO fiber-fed, multi-object spectroscopic instrument, Hydra, has been moved from the Mayall to the WIYN telescope. Modifications to the instrument allow the fibers to align with the telescope exit pupil while lying along the curved focal surface. We also upgraded the manner in which the fibers are held in place around the focal plane in order to reduce neighboring fiber interactions beyond the pivot circle. In addition, the wavelength calibration assembly was modified to take advantage of extra room within the instrument. We developed guiding algorithms which utilize the field orientation probes (7-fiber coherent bundles). The Bench Spectrograph associated with Hydra was also moved over to the WIYN. Commissioning is currently underway at the time of this paper and is expected to be complete by mid-summer of 1995. We give a general description of the instrument, discuss initial efficiency and scattered light measurements, and comment on the performance of the guider.

**Keywords:** Multi-object spectrograph, fiber optics

## 1. INTRODUCTION

Hydra, a multi-object fiber positioner and spectrograph first constructed for the Mayall 4 meter telescope,[1,2] has been reconfigured for permanent installation on the WIYN 3.5 meter telescope.[3,4] Many of the modifications for the instrument were described by Barden et al. (1994).[4] Here we describe some of the performance characteristics for the instrument which have been evaluated so far. This is not a thorough description as we are just now in the middle of the commissioning phase at the writing of this paper.

## 2. INSTRUMENT DESCRIPTION HIGHLIGHTS

Hydra is a fiber-optic, multi-object spectrograph based upon the AUTOFIB[5] concept. The instrument is located on one of the two Nasmyth ports of WIYN. Figure 1 shows the instrument as mounted at WIYN. For convenient access to the inner workings of the instrument, a hinge mechanism was devised as shown in Figure 2.

An X-Y-Z robotic positioner with a 3-fingered gripper places fibers, one at a time, onto target positions within a full 60 arc-minute diameter field of view. The dual X-stages, Y-stage, and gripper components are visible in Figure 2. A close up view of the Z-stage, gripper, gripper TV, wide field corrector, and wavelength calibration sources is shown in Figure 3.

The focal plate to which the fibers are magnetically held, once the gripper has positioned them, is warpable. This allows the fibers to be positioned onto a flat plane simplifying the robotic design. The plate is then warped against a spherical backstop by applying a vacuum to align the fibers along the focal surface of the telescope and to tilt them for alignment with the principal ray (the WIYN focal surface was designed to be nearly concentric between the 5.7 meter radius of curvature for the focal surface and the exit pupil distance of 6.9 meters).

*Operated by the Association of Universities for Research in Astronomy, Inc. (AURA) under cooperative agreement with the National Science Foundation.

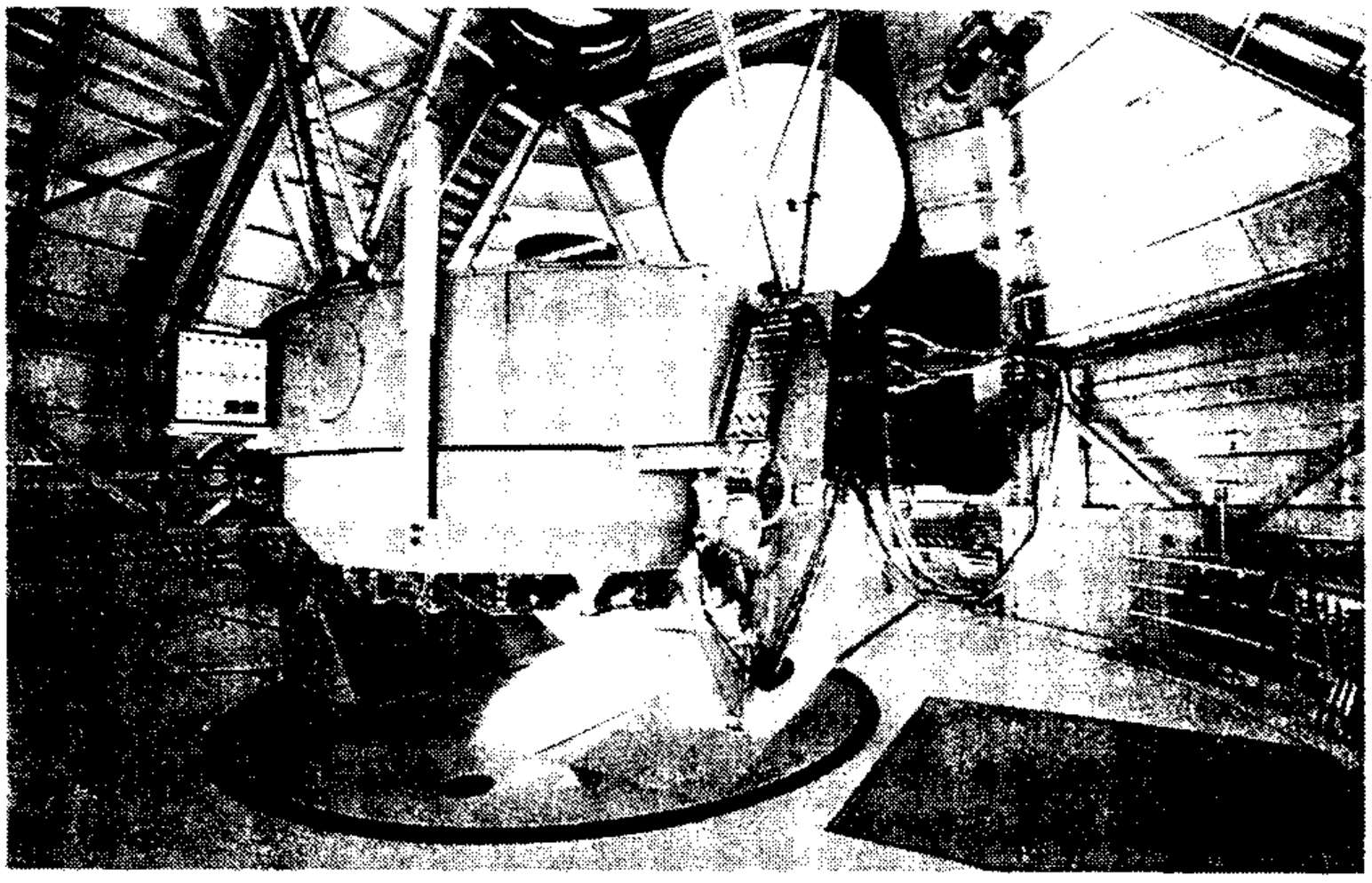

Figure 1: Hydra as mounted on the WIYN telescope.

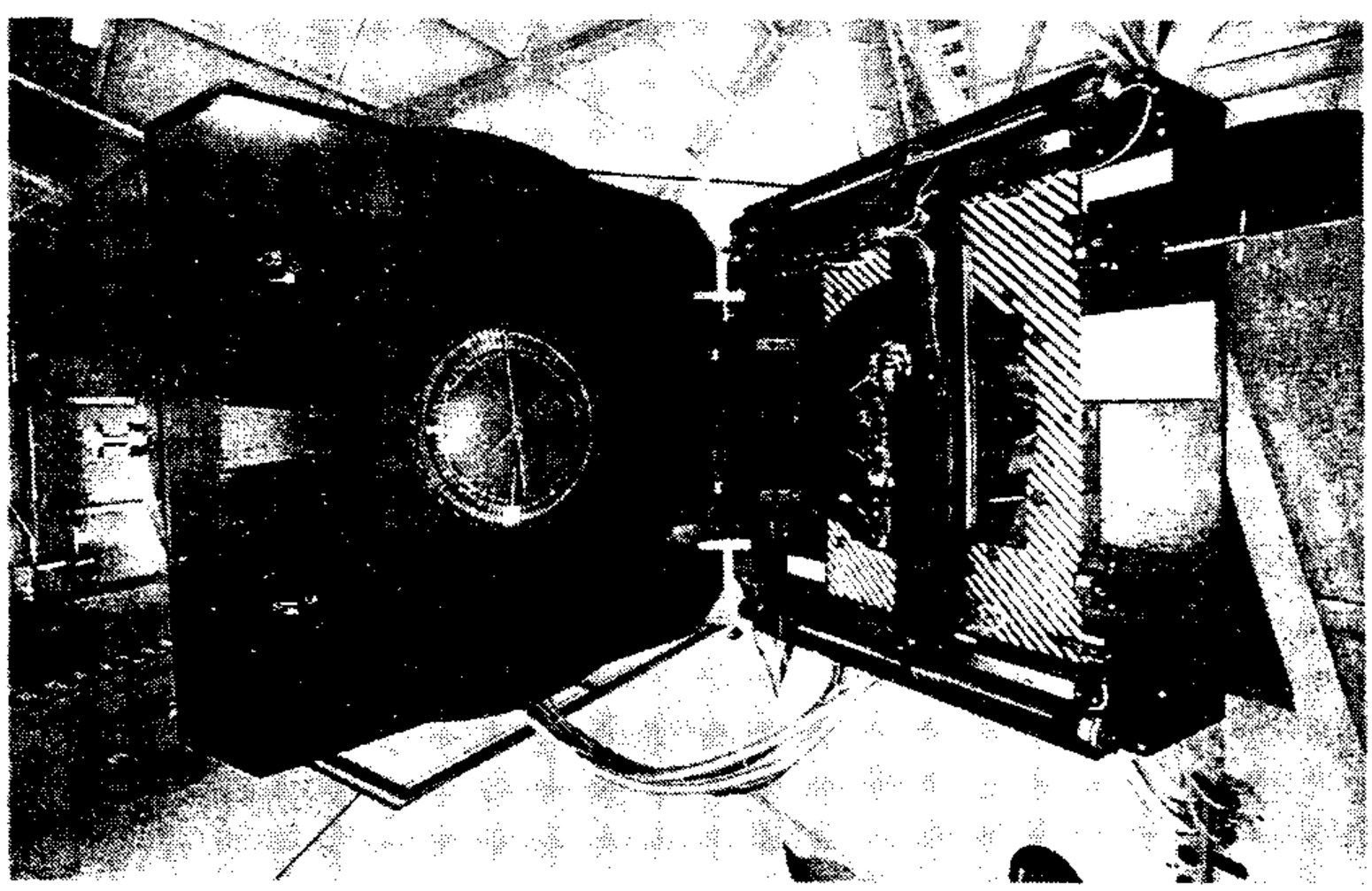

Figure 2: View of Hydra hinged open for access to the robot, focal plate, and fiber optics.

Up to 288 fibers can be installed around the focal plate assembly. The fibers currently installed include 2 science cables of 96 fibers each, one set optimized for the red with 2 arc-second diameter fibers, the other optimized for the blue spectral region with 3 arc-second diameter fibers; a set of twelve Field Orientation Probes (FOPS) which are small bundles of 7 fibers each for field acquisition and guiding. This leaves 84 empty slots for future implementation and spare fibers. Figure 4 gives a close up view of the warpable focal plate, installed fibers located at target positions on the focal plate and located in their parked positions, and the channeled grooves which help to minimize fiber to fiber interactions outside of the pivot circle (2 sectors have their aluminum tops removed). Figure 5 shows the fibers

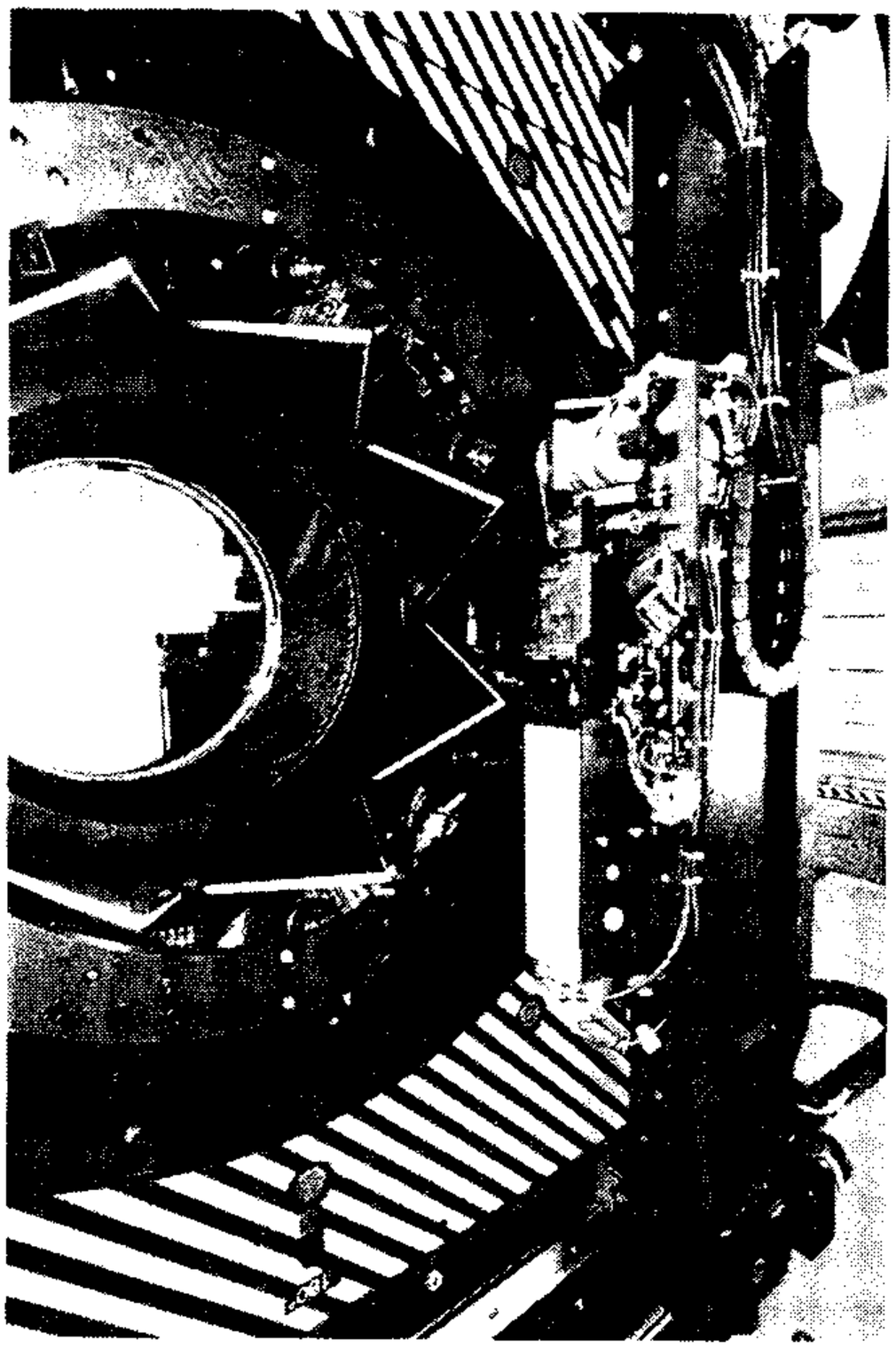

Figure 3: Close up view of the Hydra gripper. Visible are the 3 fingered gripper, Z-motor, ICCD TV which views through the gripper while simultaneously viewing the sky, wide field corrector, triangular panels of the calibration screen, and bank of hollow cathode tubes for wavelength calibration.

as they are mounted on the backside of the instrument. Each set of 96 science fibers are grouped into a flexible steel conduit which feeds through the telescope and down to the Bench Mounted Spectrograph located in a light-tight room. This spectrograph allows adjustability of the Camera-Collimator Angle, has a selection of gratings including a 316 grove/mm echelle, provides the option of 2 different cameras, and utilizes a SITe 2048 thinned CCD as a detector. An image of Th-Ar comparison lines is shown in Figure 6 along with an image of actual spectra obtained

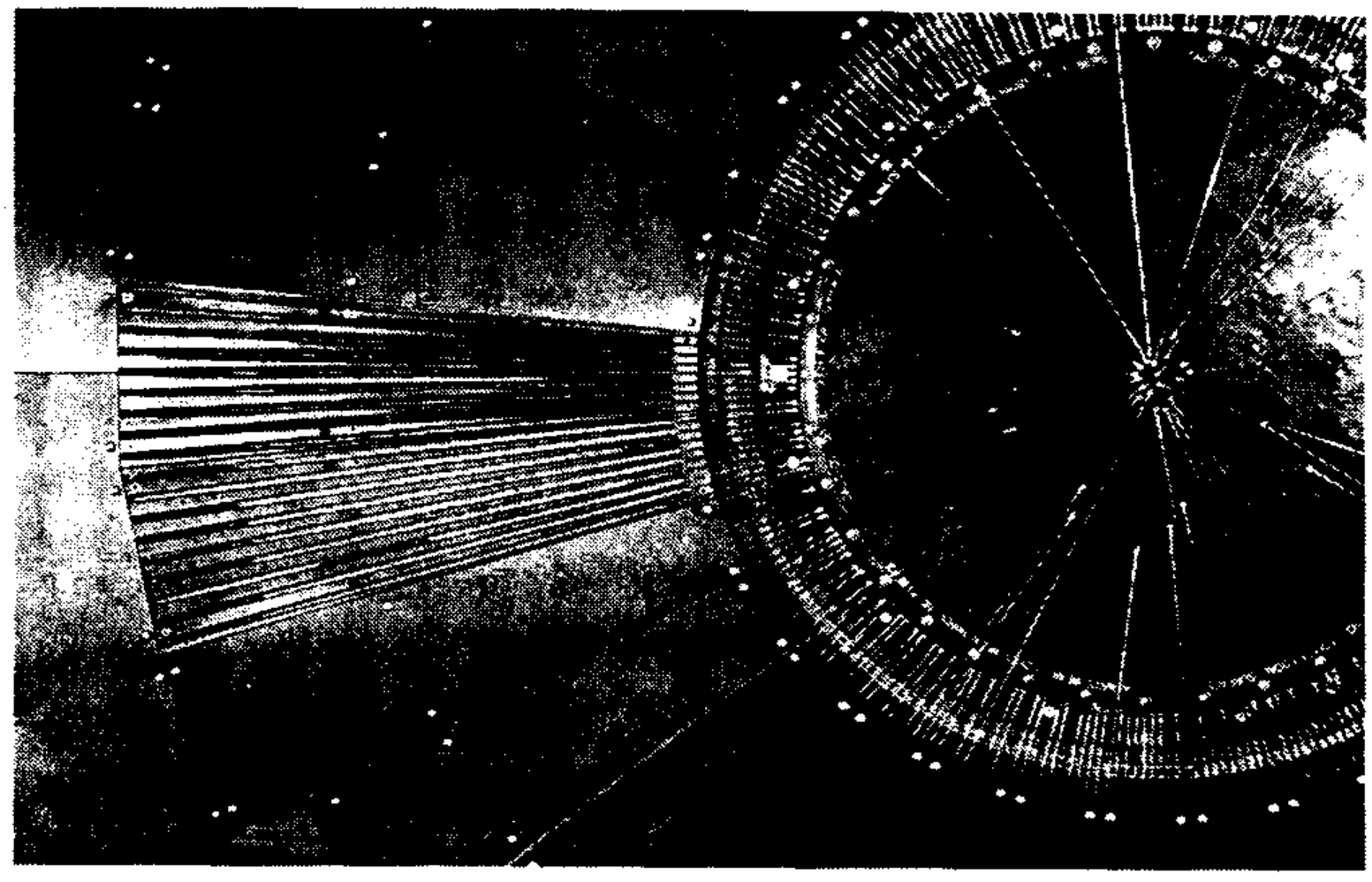

Figure 4: Close up view of the Hydra focal plate and fibers. The warpable focal plate, fibers, and channeled grooves for better fiber management are visible.

on a sample target field.

## 3. INSTRUMENT HISTORY

Hydra was first developed for use on the Mayall 4-meter telescope and was so used during the period between the fall of 1990 and the summer of 1994. The development of modifications required for installing the instrument at WIYN was a two year project. Hydra was decommissioned in July, 1994, and retrofitted with the modified components during the remainder of that summer. Photographic plates were obtained in February, 1995, shortly after installation of the wide field corrector. The plates were taken for evaluation and characterization of the astrometric solution. Hydra was installed onto the WIYN telescope in early March, 1995, for the commencement of commissioning activities. Such activities are likely to last through May and June, with shared risk science activity expected to commence by mid-summer of 1995.

## 4. WIDE FIELD IMAGING AND ASTROMETRY

The delivered image quality at WIYN is excellent. Median seeing is 0.7 arc-seconds FWHM with sub-arc-second seeing most of the time. The majority of the image quality measurements have been obtained on the Nasmyth port with the CCD imager. We believe, however, that the port with Hydra also achieves similar image quality. This can be substantiated by the following: The optical design of the corrector delivers an optical image that contains 90% encircled energy within a 0.4 arc-second diameter circle at all field radii. Some of the photographic plates taken for astrometric evaluation show an image quality of about 0.9 arc-seconds which is uniform across the full field of view. Contemporaneous CCD images obtained on-axis at both ports show that the image quality tracks between the ports to within a few-hundredths of an arc-second.

An astrometric solution was derived from a total of 10 fourteen-inch plates taken with the Lockheed camera which had a plate holder modified to match the field curvature at WIYN. Each plate had between 300 and 2200 measured stars. One set of plates were evaluated at Yale by Xinjian Guo, Terry Girard, William van Altena, and Arnold Klemola. Another set of the plates were measured at USNO by David Monet and evaluated by Phil Massey at NOAO. Solutions by both groups to the astrometric measurements gave solution residuals of better than 0.1 arc-seconds rms. All solutions were consistent with a linear plate scale plus a standard pincushion distortion term of $r(1 + 81.0r^2)$ where $r$ is the radial distance from field center in radians. The current linear plate scale that provides the best placement of fibers is 9.3950"/mm. Final adjustment of these values is underway by measuring the residual displacement of the fibers with respect to their target stars. The formal solutions from both groups also indicate that any potential asymmetry in the solution is no larger than the solution uncertainty.

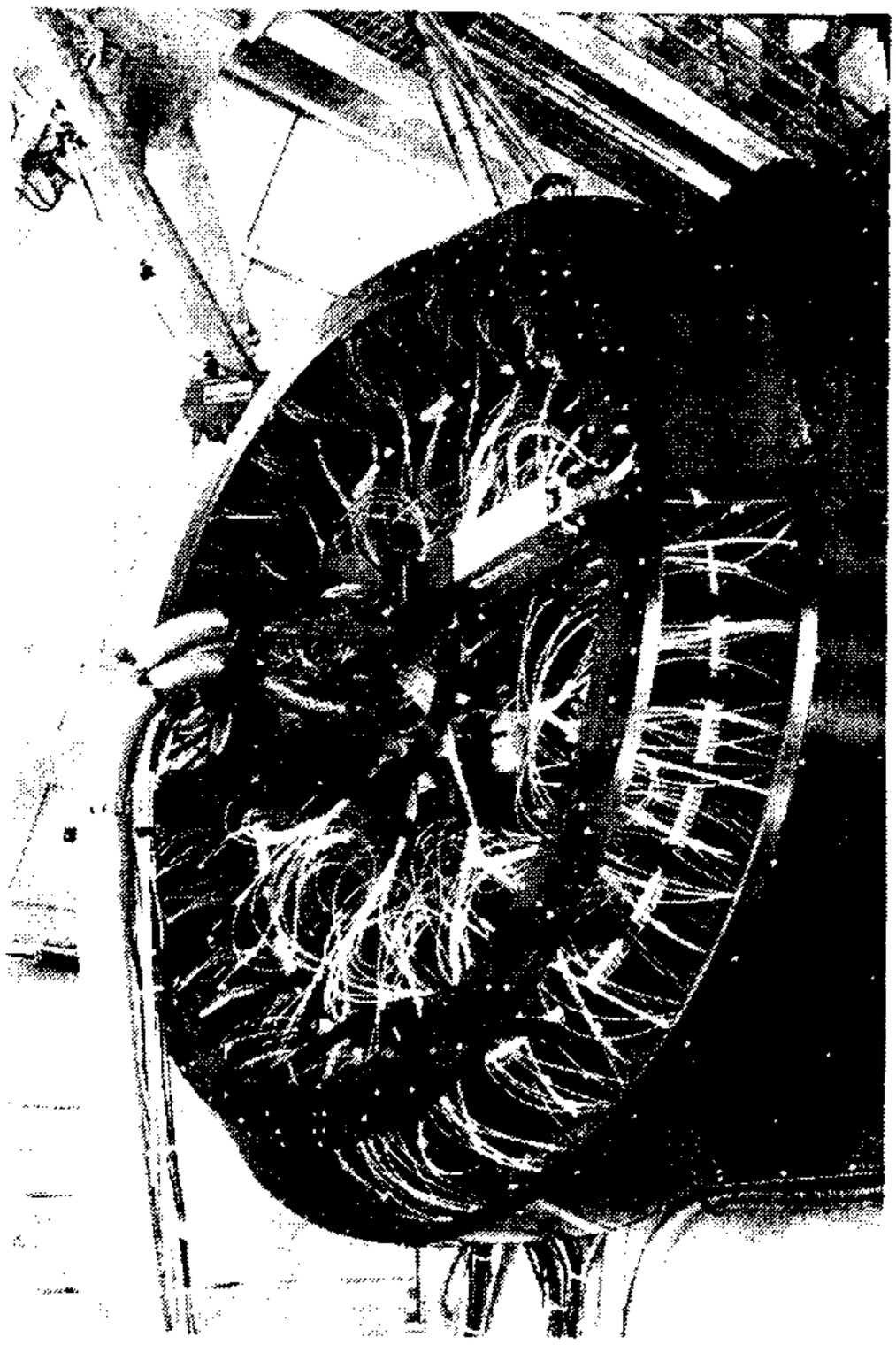

Figure 5: Backside view of the instrument with protective covers removed to show how the fibers are looped and managed. The ICCD TV which views the 12 FOPS is also visible.

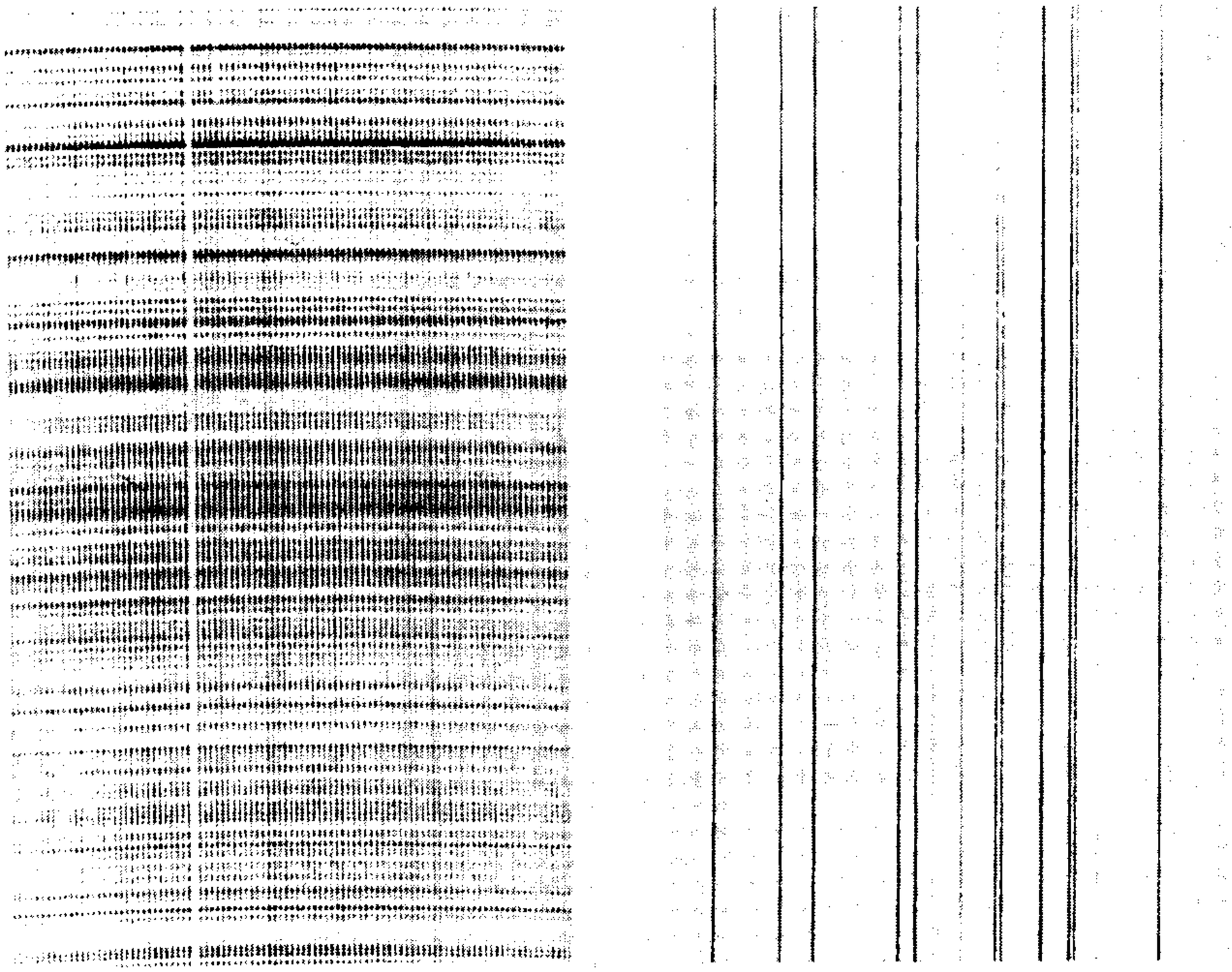

Figure 6: A Th-Ar spectrum is shown on the left. The right half of this figure shows the spectra of a sample of giant stars located in the globular cluster M71. The spectral direction runs vertically.

Residual complicating factors in placement of the fibers onto the target stars may arise from the following:

- Residual errors in measurements of the fiber concentricities (ie. alignment of the fiber within the magnetic button).
- Possible asymmetry in the geometrical fiber displacement as the plate warps.

It appears that we are placing fibers at about the 0.5 arc-second level. Refinement of the astrometric solution and exploration of the above factors should reduce residual errors to below the 0.25 arc-second level which is the measured limit in positioning accuracy for the robotic gripper assembly.

## 5. WARPED PLATE GEOMETRY

Figure 7 shows a cutaway, side view schematic of the warpable plate. As the plate warps, the fiber position is

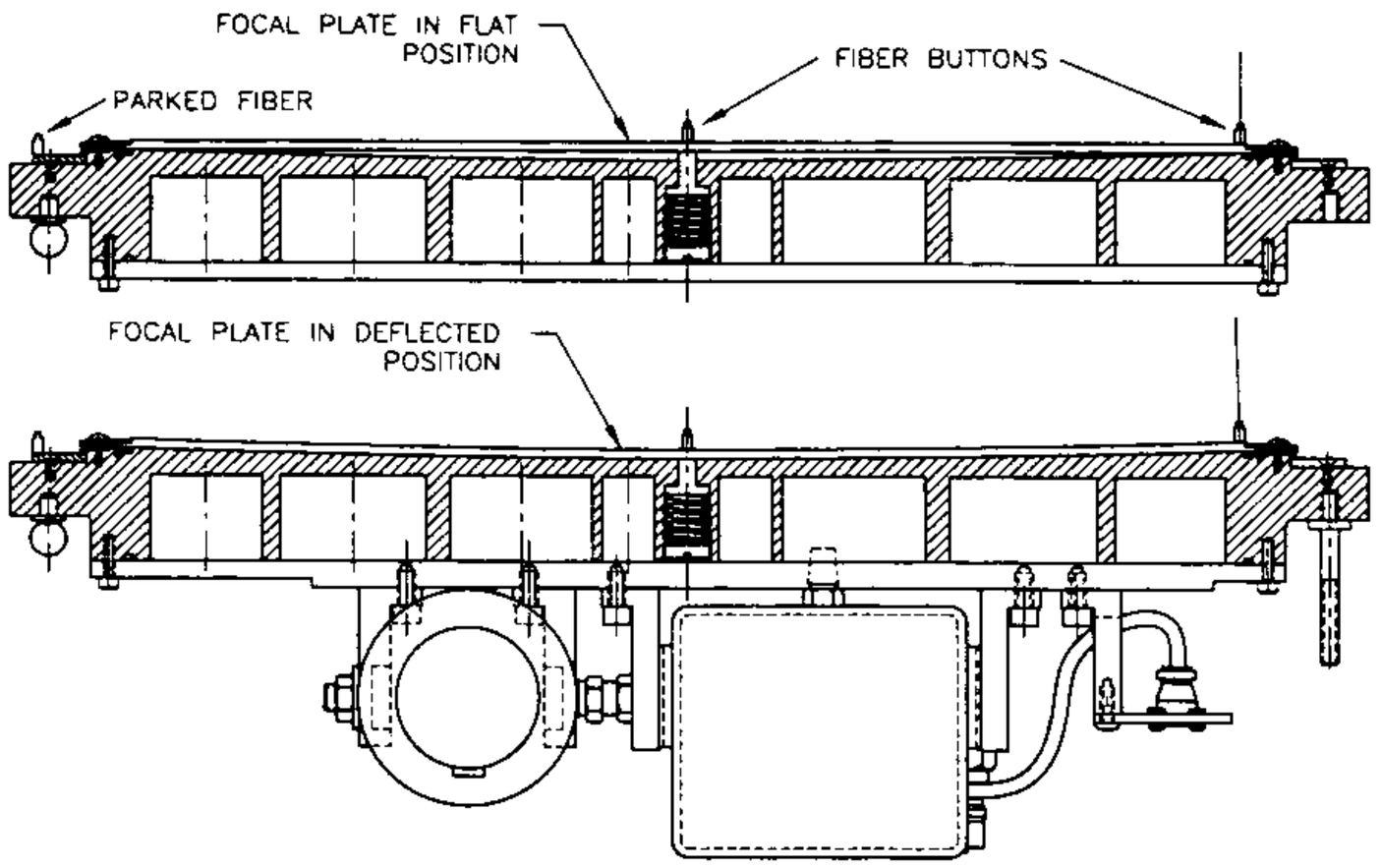


Figure 7: The warpable plate and fibers in both the flat and warped positions.

displaced towards the field center. A proper model of this displacement is required in order to accurately position the fiber onto the focal plate so that it displaces to the target position as the plate is warped.

A physical model was developed on the assumption that the middle of the plate remained at constant dimension during the elastic warp. That is, the upper surface of the plate undergoes a slight compression while the back surface of the plate experiences a stretching. The geometry simplifies to the following equations:

$$Y_{pl} = R_m \theta \tag{1}$$

$$sin(\theta) = \frac{Y_s}{R_f} \tag{2}$$

where $Y_s$ is the normal radial distance of the star from the field center in encoder units (1 encoder unit is 2.5 $\mu$m); $R_f$ is the focal surface radius; $R_m$ is the radius of the middle of the plate when it is warped; and $Y_{pl}$ is the radial distance from the plate center that the fiber will be placed onto the flat plate. Figure 8 shows this model plotted along with the measured fiber displacements for various radial distances from plate center. Note that the observed values deviate from the model near the edge of the plate where the edge clamps required to hold the plate in place

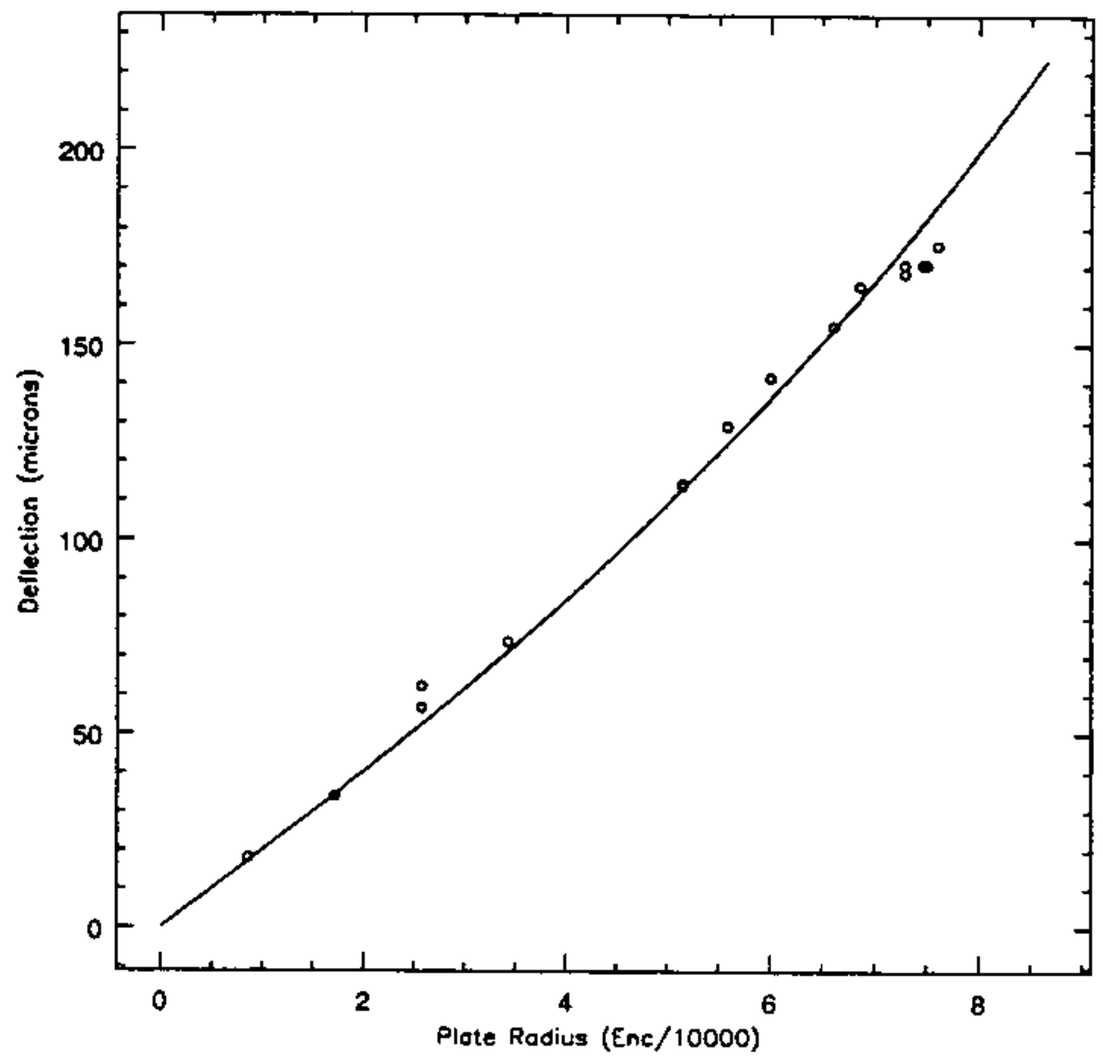


Figure 8: Theoretical model for the fiber displacement by the warped plate (solid line) with observed fiber displacements plotted by the open circles.

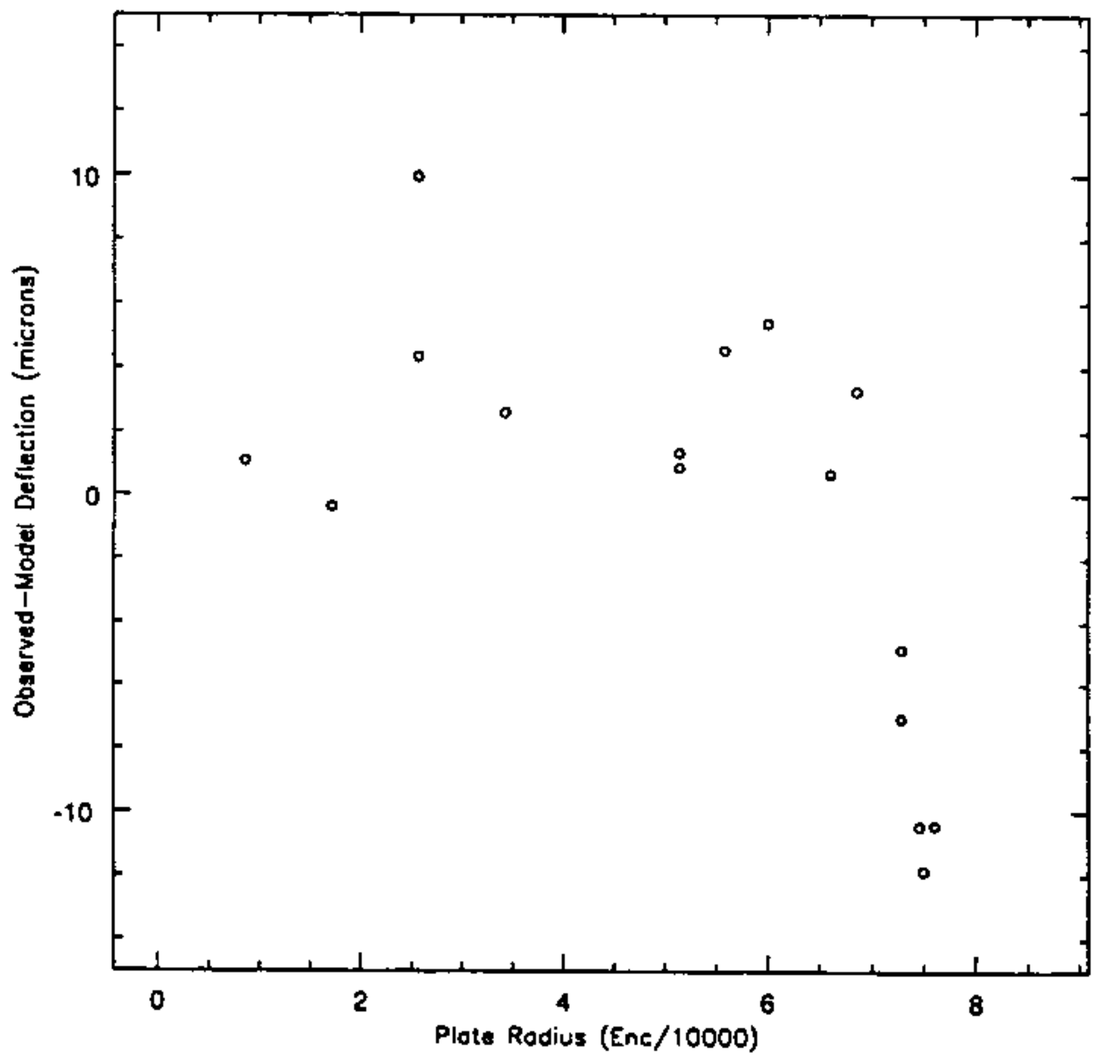


Figure 9: Residual errors in the displacement of the observed fiber minus the model prediction in microns. Note that the maximum error at the plate edge is 11 $\mu$m or about 0.12 arc-seconds.

are applying sufficient force preventing the plate from following the ideal sphere. The resultant residual errors in the predicted fiber displacement are shown in Figure 9.

A refined, empirical model based upon the above equations was produced in which the mid-radius value is held constant for the inner regions of the plate and follows a quadratic polynomial for the outer annulus. This correction to the mid-radius value is given by the following:

$$R_m = \begin{cases} 5679.881 & \text{for } r < 60773 \\ 5670.799 + r(2.988726 \times 10^{-4} - 2.458933 \times 10^{-9} r) & \text{for } r \geq 60773 \end{cases} \quad (3)$$

Figure 10 plots the derived $R_m$ values for each observed displacement and overplots the modified model.

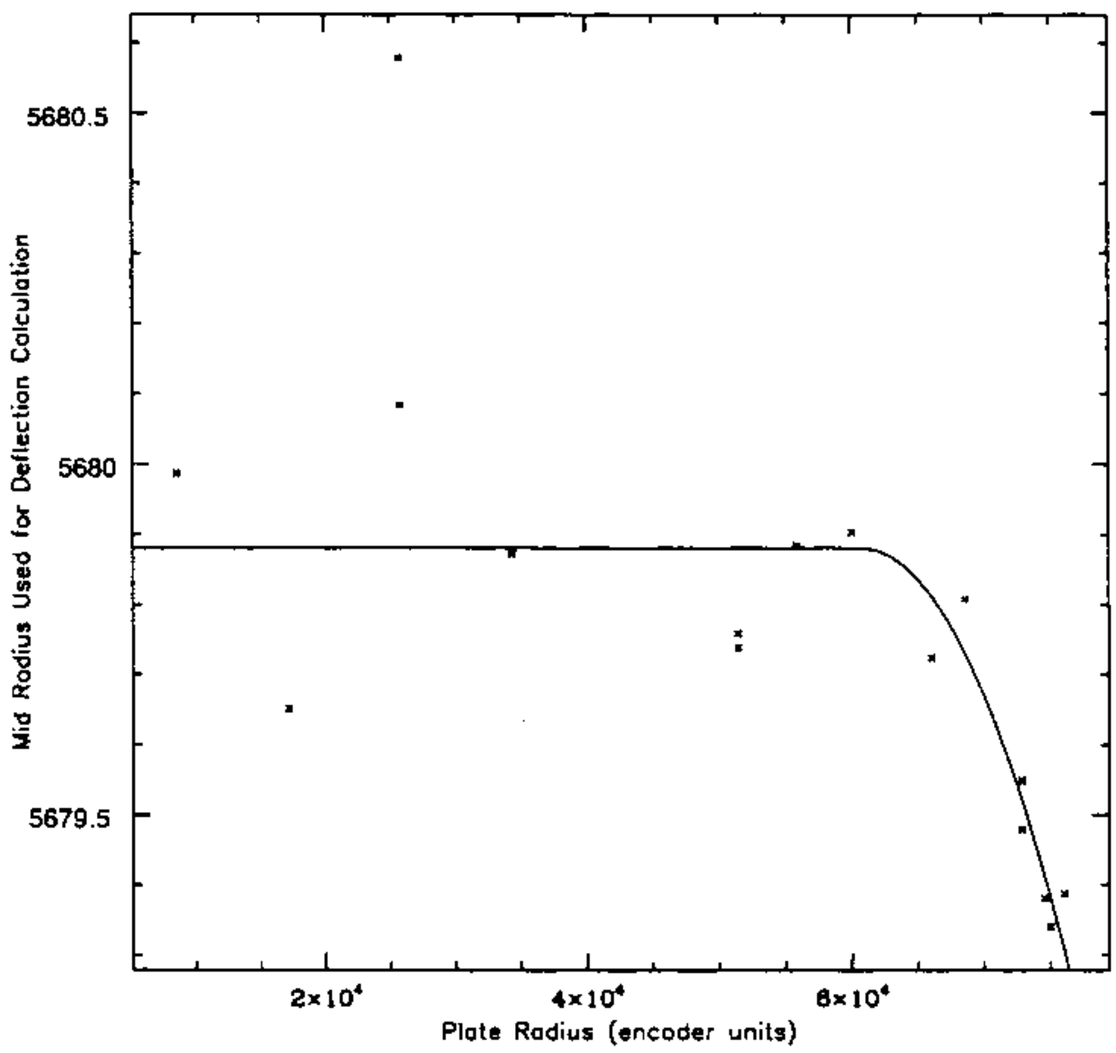


Figure 10: Plot of $R_m$ derived from the empirical observations. Observed data are shown by the crosses. The new model for $R_m$ is indicated by the solid line.

The data used to compute the empirical model were averages over azimuth about the plate center. There is possible evidence for some asymmetry in the geometrical displacement about plate center, however, further investigation is required and underway to determine if such systematic errors exist. If so, this may explain some of the residual astrometric errors.

## 6. SYSTEM EFFICIENCY

We are in the process of evaluating the overall system efficiency. The numbers currently indicate that the efficiency is consistent with that observed when Hydra was at the Mayall 4-meter. Peak system efficiency is probably between 3 and 5% with the Simmons camera which has a 40% central obstruction. We expect that the new refractive bench camera will improve overall efficiency by nearly a factor of two since it has both a higher transmissive efficiency than the Simmons and it is an all transmissive camera without any central obstructions. The new camera will only be used for observations redward of 3800 Å due to the blue cutoff of the glasses and coatings used. The Simmons will see continued use for observations blueward of that cutoff.

## 7. BACKGROUND LIGHT

Hydra's tenure at the 4-meter was slightly compromised by the presence of background light contamination arising from two sources:

- The presence of phosphorescent materials in the spectrograph room.
- Inherent scattering of light within the spectrograph.

This contamination sometimes impacted the signal to noise of the observed spectra and handicapped the ability to do high precision sky subtraction if it wasn't properly removed during the data reduction process.

At the WIYN, we took a vigilant approach to minimize such background light. A study was conducted to detect any phosphorescent materials which were then replaced with non-phosphorescent items. We found the following sources of phosphorescence:

- Most wall paints. Flat black was used to eliminate this source.
- Most floor tiles. Again, we found a black floor tile which wasn't phosphorescent.
- Plastic light switch panels. Replaced with metallic panels.
- Glass panels in the incandescent ceiling light fixtures. We removed those panels.

In addition, we found leaky fiber optic connectors in the CCD controller which we corrected by encasing them in a light-tight box. There are also some fiber cable jackets which are not completely opaque to leaking light from the fiber. Fortunately, our controller fiber optic cables themselves do not leak.

To minimize inherent scattered light in the spectrograph, we added black velvet flocking to some of the likely surfaces of reflection. At the 4-meter, we had only roughened those surfaces prior to anodizing them black. We also have implemented masking around each grating for further scattered light reduction.

Our current measurements indicate that we have reduced the level of background light by at least a factor of two from that experienced at the 4-meter. Light contamination from phosphorescence is now effectively zero within a few minutes after the room lights are turned off. Peak scattered light for the worst case is about 0.01% of the signal for a star illuminating a single fiber. In the majority of grating configurations, the scattered light level is significantly lower than this worst case value. In comparison, spectra obtained at the 4-meter were showing scattered light values of up to 0.03%.

## 8. HYDRA GUIDER

For closed-loop guiding of the telescope, we are utilizing probes each consisting of a bundle of 7 hexagonally packed fibers which we call Field Orientation Probes or FOPS. The FOPS are placed on target stars in the same manner as the science fibers. Similar probes were used on Nessie[6] and on Hydra at the Mayall telescope[2] for alignment on the target field. A schematic representation of a FOP is shown in Figure 11. There are a total of twelve FOPS equally spaced around the focal plate. At least 2 FOPS are assigned in a target field to allow rotational alignment as well as translational alignment in RA and Dec.

Simulations of the basic centroiding algorithm, which computes the first moment of the signal coming through the seven fibers, show that we can produce a centroid with fairly good accuracy for the majority of seeing conditions at WIYN. Figure 12 shows those simulations of the computed centroid versus the position of a simulated star on a simulated FOP.

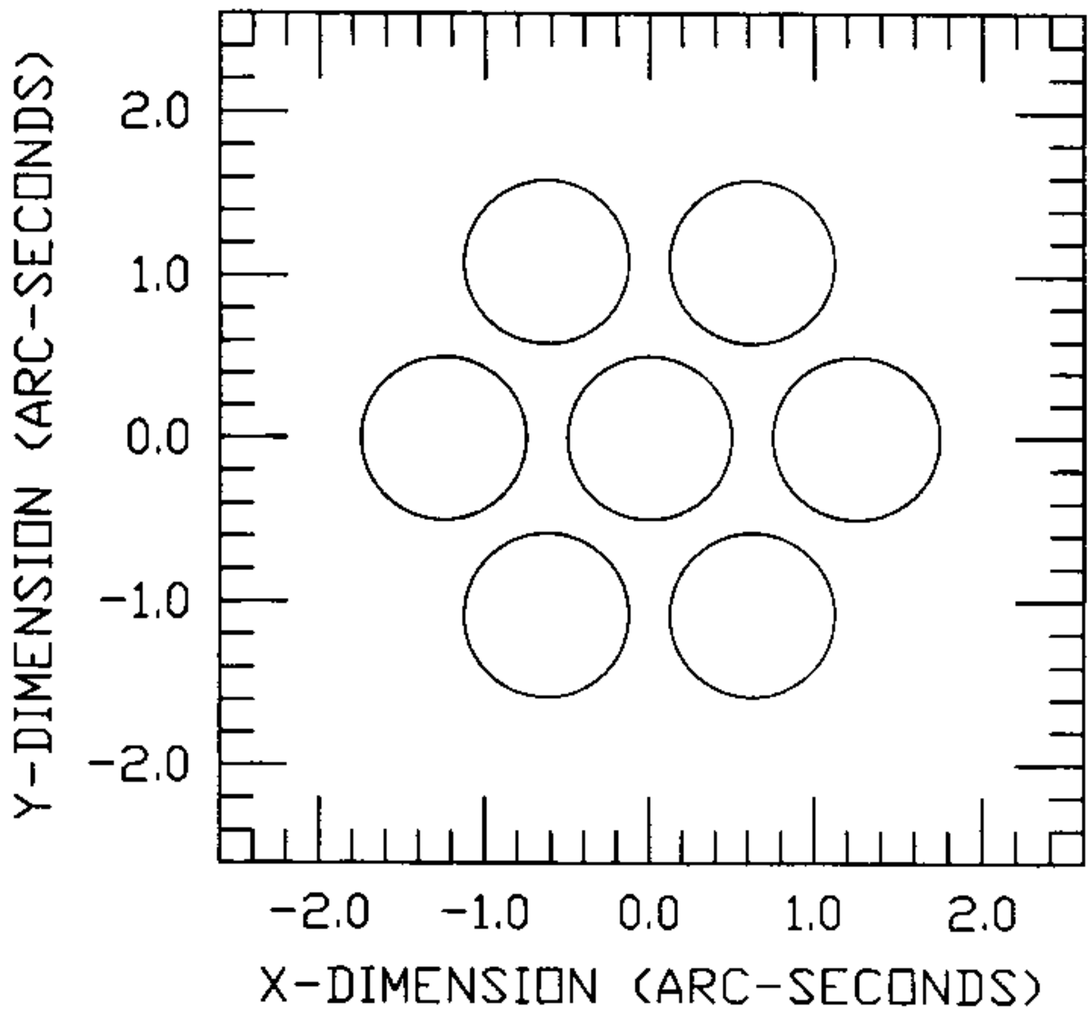


Figure 11: Schematic layout of the fibers in a single field orientation probe (FOP).

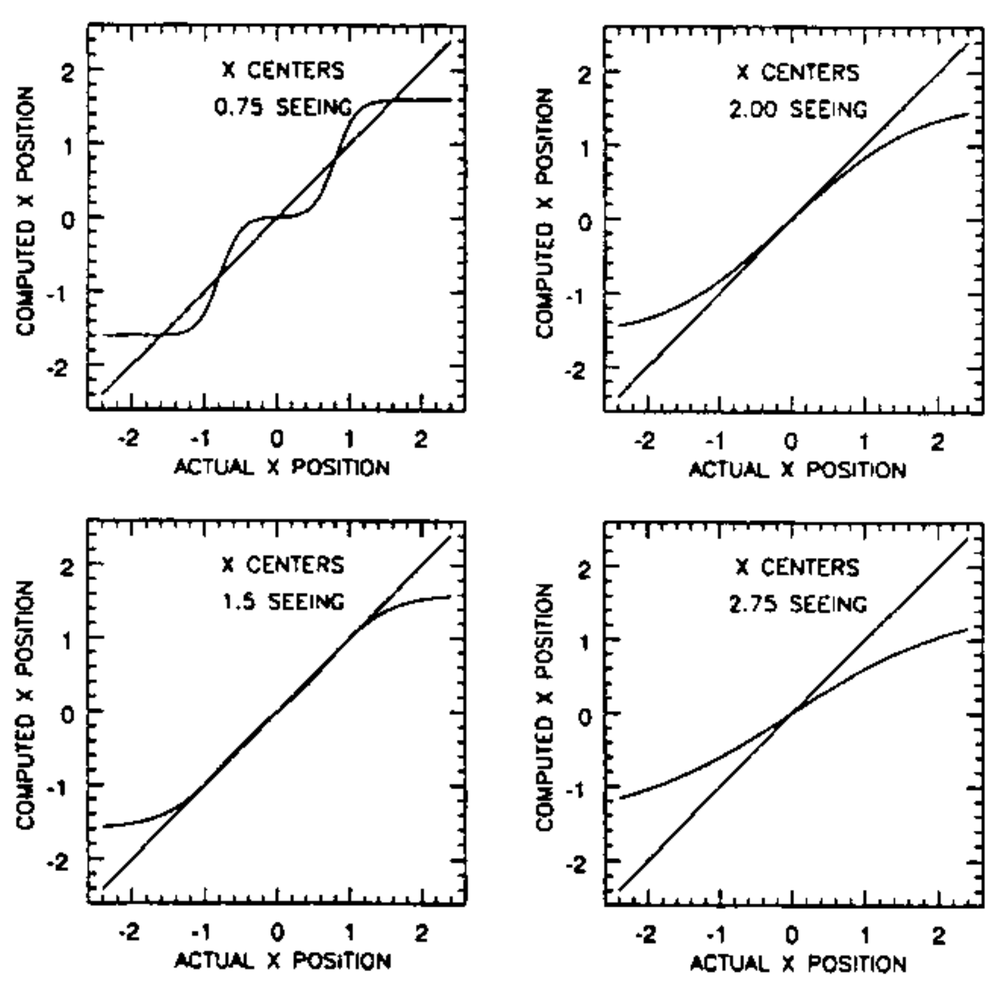


Figure 12: Computed centroid versus position of a simulated star shifted along the X-axis of the FOP for a variety of seeing conditions.

The actual performance of the guider is quite good. Although we are still evaluating its level of performance, we note that it is able to hold the telescope to within 0.25 arc-seconds when guiding on 11th magnitude stars. We have also verified that guiding is still quite good when using stars as faint as V=16 in full moon sky conditions.

## 9. OUTLOOK

As mentioned above, we hope to begin shared risk science operation sometime this summer. Given the excellent image performance of the telescope, we hope to eventually implement smaller core fibers (1 to 1.5 arc-second) to take advantage of that image quality for the observation of faint, point-like sources where the smaller fiber can suppress more of the background sky. This would allow us to observe 1-2 magnitudes fainter before potential sky subtraction limitations start compromising the data.

Hydra at WIYN should easily remain a competitive workhorse instrument well into the 21st century.

## 10. REFERENCES


1. S. C. Barden and A. C. Rudeen, "Kitt Peak National Observatory fiber actuator device", Instrumentation in Astronomy VII, ed. D. L. Crawford, Vol. 1235, pp. 729-735, SPIE, Tucson, 1990.

2. S. C. Barden, T. Armandroff, P. Massey, L. Groves, A. C. Rudeen, D. Vaughnn, and G. Muller, "Hydra – Kitt Peak Multi-Object Spectroscopic System", Fiber Optics in Astronomy II, ed. P. M. Gray, Vol. 37, pp. 185-202, ASP, Sydney, 1993.

3. M. W. Johns and D. R. Blanco, "WIYN 3.5-meter telescope project", Advanced Technology Optical Telescopes V, ed. L. M. Stepp, Vol. 2199, SPIE, Kona, 1994.

4. S. C. Barden, T. Armandroff, G. Muller, A. C. Rudeen, J. Lewis, and L. Groves, "Modifying Hydra for the WIYN telescope – an optimum telescope, fiber MOS combination", Instrumentation in Astronomy VIII, ed. D. L. Crawford and E. R. Craine, Vol. 2198, pp. 87-97, SPIE, Kona, 1994.

5. I. R. Parry and P. M. Gray, "An automated multiobject fibre optic coupler for the AAT", Instrumentation in Astronomy VI, ed. D. L. Crawford, Vol. 627, pp. 118-124, SPIE, Tucson, 1986.

6. S. C. Barden and P. Massey, "Nessie – A Versatile Multi-fiber Feed on the KPNO Mayall 4-Meter Telescope", Fiber Optics in Astronomy, ed. S. C. Barden, Vol. 3, pp. 140-152, ASP, Tucson, 1988.